Pullout capacity of horizontal circular plates embedded in sand using the method of stress characteristics

Majd Tarraf & Ehsan Seyedi Hosseininia

Taylor & Francis
Taylor & Francis Group

Check for updates

Pullout capacity of horizontal circular plates embedded in sand using the method of stress characteristics

Majd Tarraf and Ehsan Seyedi Hosseininia

Civil Engineering Department, Ferdowsi University of Mashhad, Mashhad, Iran

ABSTRACT

The pullout capacity of horizontal anchor plates plays a crucial role in ensuring the stability and performance of various structures subjected to uplift or lateral loading. This paper presents an investigation into the pullout capacity of horizontal anchor plates using the method of stress characteristics. The method offers a simplified analytical approach that allows for quick estimations and insights into the stress distribution and failure mechanism of anchor plates. The study focuses on circular anchor plates with varying embedment ratios, considering different soil friction angles. Through computational analyses and the generation of characteristic grids, the behavior and stress distribution of anchor plates are examined. The results are compared with several experimental data from the literature to validate the applicability of the method. The findings provide valuable insights into the influence of embedment ratios and soil friction angles on the pullout capacity of horizontal anchor plates. This research contributes to the understanding of anchor plate behavior and offers a practical tool for assessing their performance in geotechnical engineering applications.

1. Introduction

Horizontal anchor plates play a crucial role in providing resistance against uplift in various structural systems. These plates are designed to harness the high passive resistance offered by the surrounding soil, allowing them to effectively transfer and distribute applied loads. Horizontal anchor plates find wide application in stabilizing structures such as transmission towers, buoyant pipelines, wind-resistant towers, and mooring systems in the onshore and offshore industry (Ganesh and Sahoo 2019; Mariupol'skii 1965; Mohammadkhanifard et al. 2022; Rowe and Davis 1982; Xing et al. 2023; Zhang et al. 2017). However, accurately determining the pullout capacity of horizontal anchor plates remains a complex challenge in geotechnical engineering. It requires a comprehensive understanding of the soil-plate interaction, considering factors such as soil properties, embedment depth, and plate geometry. The behavior of horizontal anchor plates embedded in sand is influenced by the interplay between the soil and the plate, as well as the failure mechanisms associated with the pullout process. Precisely assessing the pullout capacity is essential for ensuring the structural stability and safety of the supported systems. Therefore, advancing the knowledge and addressing the challenges related to the pullout capacity of horizontal anchor plates is of paramount importance in the field of geotechnical engineering.

In the literature review of the horizontal anchor plate embedded in cohesionless granular materials such as marine sand, there is a wide range of research in which different approaches have been applied. Experimental studies including small-scale (Clemence and Veesaert 1977; Mitsch and Clemence 1985; Mittal and Mukherjee 2014; Mohammadkhanifard et al. 2022; Sabermahani and Shojaee Nasirabadi 2021) and centrifuge tests (Dickin 1988; Dickin and Leung 1983) have been performed in which, different depths and shapes were investigated. Besides, analytical and numerical methods have been widely used. Since these methods are always accompanied by several assumptions and input variables such as soil failure mechanism, soil characteristics (shear strength and mechanical properties), soil model behavior (e.g., hardening, softening), embedment depth, rigidity and geometry of plates, etc, the validity is highly dependent on the agreement with experimental results. Analytical methods include limit equilibrium (Balla 1961; Mariupol'skii 1965; Meyerhof and Adams 1968), limit analysis (Hu et al. 2022; Merifield, Lyamin, and Sloan 2006; Merifield and Sloan 2006; Zhao et al. 2011), and method of characteristics (Kanakapura, Rao, and Kumar 1994). In addition, numerical methods are used for the study of anchor plates majorly including finite element and finite different methods (Al Hakeem and Aubeny 2019; Kumar 2006; Mokhbi et al. 2018; Xing et al. 2023) in the domain of continuum mechanisms and recently multiphase/discrete element method (Liang et al. 2021; Zhang et al. 2020). Numerical simulation methods offer a detailed analysis of anchor plate behavior and soil interaction, accommodating complex geometries and non-linear soil properties. For instance, by

CONTACT Ehsan Seyedi Hosseininia ✉ eseyedi@um.ac.ir 🖃 Civil Engineering Department, Ferdowsi University of Mashhad, Mashhad, Iran.
🌐 https://prof.um.ac.ir/eseyedi

implementing the finite element method, Al Hakeem and Aubeny (2019) investigated the rigidity of the plate as well as the soil dilation angle on the pullout capacity. Numerical methods have the ability to capture displacement fields of the soil around the anchor too and to obtain the load-displacement response of the anchor plate. However, they require advanced modeling skills, computational resources, and can be time-consuming. Limit equilibrium methods provide quick estimations accompanied by simple calculation process but their assumptions and simplified failure surface representation may limit accuracy for complex cases. Limit analysis, on the other hand, offers rigorous upper bound solutions (by assuming statically admissible stress field) and considers plastic deformation (by assuming dynamically admissible displacement fields) in the soil, but it requires specialized software and may provide conservative estimates. The choice of method depends on project requirements, available resources, and desired accuracy, often involving a combination of methods for initial estimations and detailed analysis.

The method of stress characteristics, also known as the slip-line method, offers several advantages over other commonly used methods in geotechnical engineering. It provides a simplified analytical approach for estimating the pullout capacity of anchor plates, offering insights into stress distribution and failure mechanisms. This method is versatile, applicable to both cohesive and cohesionless soils, and does not require complex modeling techniques or extensive computational resources. Compared to limit equilibrium methods, the stress characteristics method provides more detailed stress fields, allowing for a comprehensive analysis of stability and failure modes. While limit analysis offers rigorous upper-bound solutions, the slip-line method is useful for preliminary analyses to assess potential failure mechanisms. The method of stress characteristics, as proposed by Sokolovski (1965), is considered as a standard calculation procedure in geotechnical engineering. It solves for plastic equilibrium in the vicinity of the applied load, avoiding arbitrary slip surface assumptions. The method produces zones where equilibrium and plastic yield are simultaneously satisfied for given boundary stresses. Compared to limit analysis, the method of stress characteristics provides a direct problem solution, while the limit analysis yields a range of solutions based on bound limits. According to Bolton and Lau (1993), this approach strikes a balance between the simplicity of limit equilibrium methods and the computational complexity of numerical methods.

By reviewing the literature, the applicability of the method of stress characteristics in predicting the pullout capacity of horizontal anchor plates has been demonstrated in only one work. Kanakapura, Rao, and Kumar (1994) conducted an analysis of pullout capacity for shallow strip horizontal anchor plates, assuming a log-spiral shearing surface through the soil. Their results, presented in graphs, showed that the proposed analysis provided slightly more conservative predictions of pullout capacity for cohesionless soils compared to the analysis proposed by Meyerhof and Adams (1968). This highlights the potential of the method of stress characteristics to enhance geotechnical engineering analyses and contribute to improved estimations of pullout capacity.

Overall, the method of stress characteristics offers a simplified yet effective approach to estimate the pullout capacity of anchor plates. Its versatility, detailed stress fields, and direct problem solutions make it a valuable tool in geotechnical engineering. The successful application of the method in predicting pullout capacity further validates its usefulness and potential for enhancing geotechnical engineering analyses.

Bearing in mind that the behavior of circular anchor plates is generally less investigated in comparison to square or strip anchor plates in the literature, the objective of this study is to assess the pullout capacity of horizontal circular anchors at varying embedment depths using the method of stress characteristics. By exploiting the inherent symmetry of circular plates, the analysis is formulated symmetrically. The obtained results are critically evaluated by comparing them with experimental findings reported in the literature, thereby examining the applicability and reliability of the derived outcomes. This investigation aims to contribute to the existing knowledge base and enhance understanding regarding the pullout behavior of circular anchor plates, facilitating improved design and analysis practices in geotechnical engineering applications.

2. Methodology

2.1. The method of stress characteristics in axisymmetric condition

For the problems in which, the material is in the plastic state, it is possible to find the stress tensor (or stress components) by considering simultaneously the equations of equilibrium and the yield criterion defined in terms of stress components. As a result, three sets of first-order partial equations are involved in the analysis. The method of stress characteristics is a mathematical technique to solve these three sets of equations, which results in the determination of stress components. By the method, it is shown that the equilibrium among stress components is satisfied over two intersecting lines (or characteristics). The method of stress characteristics was initially proposed for plain strain condition (Hill 1950). Its successful application to the axisymmetric problems like circular footings was first made by (1955) for Tresca (cohesive) materials and later by Cox (1962; Cox, Eason, and Hopkins 1961) for Mohr-coulomb (frictional-cohesive) materials.

According to Figure 1, consider the stress field of an element in an axisymmetric coordinate system (r-z) where r and z represent the radial and depth distance from the axis of symmetry. The stress components of the element are vertical stress (σ_z), radial stress (σ_r), hoop stress (σ_θ), and shear stress components over intersecting surfaces that are equal $(\tau_{rz} = \tau_{zr})$. The equilibrium equations under axisymmetric condition appear in the following form:

$$\begin{cases} \dfrac{\partial \sigma_r}{\partial r} + \dfrac{\partial \tau_{rz}}{\partial z} + \dfrac{\sigma_r - \sigma_\theta}{r} = 0 \\ \dfrac{\partial \tau_{rz}}{\partial r} + \dfrac{\partial \sigma_z}{\partial z} + \dfrac{\tau_{rz}}{r} = \gamma \end{cases} \tag{1}$$

where γ is the unit weight of the soil in the z-direction.

In the present work, it is assumed that the soil obeys the Mohr-Coulomb failure criterion as a frictional-cohesive material with the internal friction angle (ϕ) and cohesion (c) parameters. For a soil element with stress components ($\sigma_z, \sigma_r, \tau_{rz} = \tau_{zr}$) and based on the Mohr stress circle definition, the location of the pole as well as the major principal stress (σ_1) can be obtained according to Figure 2(a). The radius of the Mohr circle equals $R = c\cos\phi + p\sin\phi$, where p is the center of the Mohr circle $\left(p = \frac{\sigma_r + \sigma_z}{2}\right)$. The three stress components $\sigma_z, \sigma_r, \tau_{rz}$ can be expressed in terms of p and the inclination angle (ψ) between the major principal surface and the horizontal direction:

$$\begin{cases} \sigma_r = p(1 + \sin\phi\cos 2\psi) + c\cos\phi\cos 2\psi \\ \sigma_z = p(1 - \sin\phi\cos 2\psi) - c\cos\phi\cos 2\psi \\ \tau_{rz} = (c\cos\phi + p\sin\phi)\sin 2\psi \end{cases} \quad (2)$$

In axisymmetric problems, it is generally supposed that the hoop stress (σ_θ) is either the major or minor principal stress (Haar and von Karman 1909). In this work, following
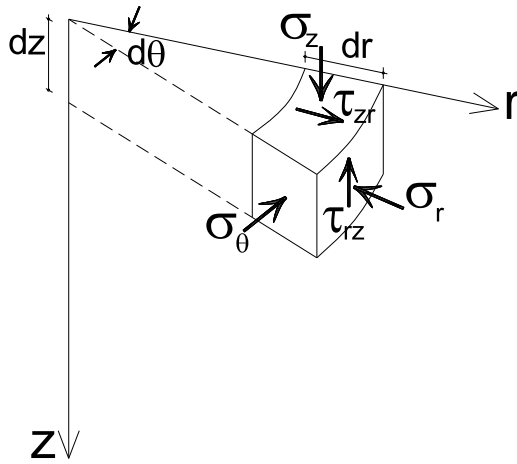

Figure 1. Presentation of a soil element with stress components in an axisymmetric coordinate system.

similar works to the bearing capacity of circular footings (Bolton and Lau 1993; Cassidy and Houlsby 2002; Kumar & Ghosh 2005; Larkin 1968), the hoop stress is considered as minor principal stress:

$$\sigma_\theta = p(1 - \sin\phi) \quad (3)$$

Considering Equations (1) through (3) together and searching for a unique solution for the resulting set of hyperbolic partial differential equations, two groups of characteristic lines are obtained:

$$\frac{dr}{dz} = \tan(\psi \mp \mu) \quad (4)$$

where $\mu = \pi/4 - \phi/2$. The upper and lower signs correspond to α and β lines, respectively, as shown in Figure 2. Along each of these two lines, the equilibrium is satisfied for stress components. By substituting Equation (4) into Equation (1), the set of partial differential equations reduces to two ordinary differential equations expressing the variation of mean stress (p) along α and β lines in terms of inclination angle (ψ) and the position (r, z) as shown in Figure 2(b):

$$dp\cos\phi \mp R\left(2d\psi + \frac{\cos\phi\,dr \mp (1-\sin\phi)dz}{r}\right)$$
$$- (\mp\sin\phi\,dr - \cos\phi\,d)\gamma = 0 \quad (5)$$

Again, the upper and lower signs correspond to α and β lines, respectively.

2.2. Problem definition

According to Figure 3(a), consider a circular anchor plate with a diameter D which is embedded at the depth of H from the ground surface. The thickness of the plate is ignored. The soil is cohesionless ($c = 0$) with the unit weight of γ and friction angle ϕ. It is assumed that the interface friction angle between the plate and the soil is zero. According to the results of numerical studies performed by Merifield and Sloan (2006), the interface
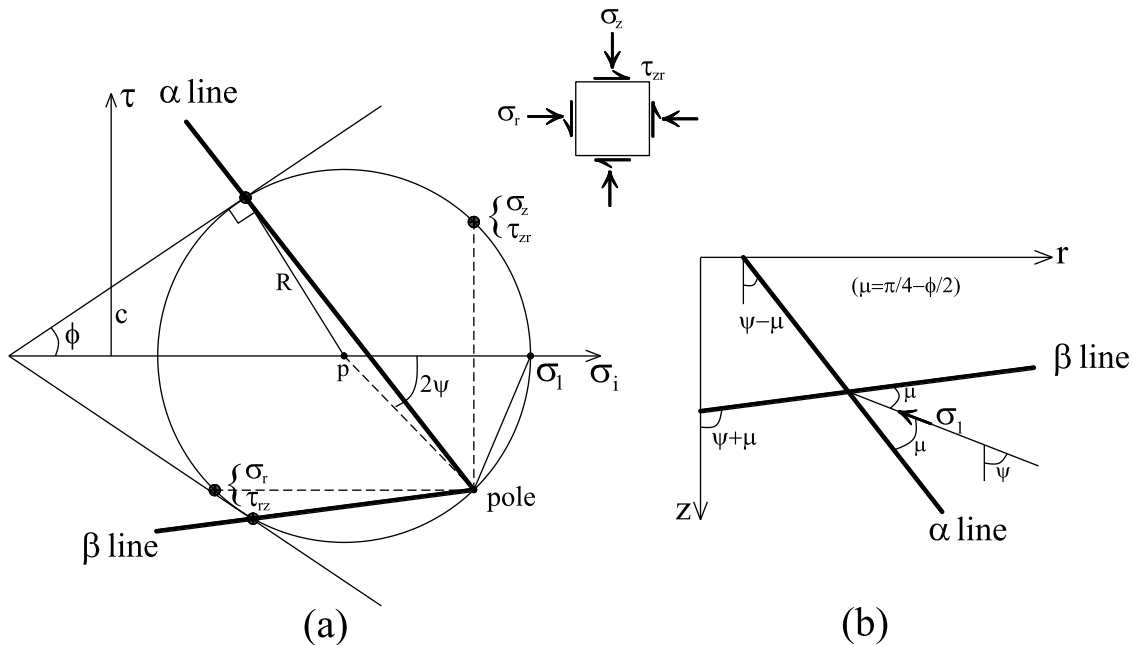

Figure 2. Presentation of two stress characteristics (α and β lines) of a soil element in the space of (a) Mohr stress circle; (b) axisymmetric coordinate system (r-z).

roughness was found to have little or no effect (less than 4%) on the pullout capacity of horizontal anchors and for the simplicity, the plate roughness is ignored in this study. As for the rupture surfaces in the soil when the anchor is loaded at the ultimate tensile load, for simplicity, it is assumed that a failure surface in the form of a straight line be generated around the anchor plate at the anchor edge. In other words, the rupture surface under the ultimate pullout loads is a truncated cone with the plate as its base. There are several values proposed for the inclination angle (α) of the slant height of the cone in the literature based on field or experimental tests. For instance, Balla (1961) considered the angle α to be 45-ϕ/2. Generally, Balla's theory agreed well with dense sand; however, it overestimates the uplift capacity for loose to medium sand. Based on the work of Meyerhof and Adams's theory (Meyerhof and Adams 1968) which resulted from the analysis of experimental tests, they found that the magnitude of the angle α depends on several factors such as the soil compaction and the soil friction angle and it varies between 90-ϕ/3 to 90-2ϕ/3 with an average of $\alpha = 90$-ϕ/2. Based on laboratory model tests, Ghaly, Hanna, and Hanna (1991) suggested that the rupture surface under the ultimate pullout loads is a truncated cone whose slant height is included at 90-ϕ/3. In another experimental work by Mitch and Clemence (1985), it is found that the inclination angle of the slant height equals 90-ϕ/2. The same value was already reported by Clemence and Veesaert (1977). The experimental investigation on relatively large-scale circular plate anchors was performed by Ilamparuthi, Dickin, and Muthukrisnaiah (2002) also showed that the average value of α is equal to 90-ϕ/2 in the case of loose and dense sand. Note that this truncated cone was generally observed for shallow anchor plates to around H/$D < 6$ and for deeper anchor plates, the failure surface does not reach the ground surface. An experimental study on the influence of soil density on the displacement field around the circular anchor plate was performed by Liu, Liu, and Zhu (2012). In addition, a comparative study on the sliding/failure surface morphology around an anchor is presented by Hu et al. (2023). In this paper, the magnitude of α angle is assumed to be equal to 90-ϕ/2 for all values of the soil friction angle irrespective of the anchor plate depth.

To differentiate between the behavior of shallow anchors from deep anchor plates, the critical embedment ratio (H/D)$_{cr}$ is defined. Experimental investigations show that the ultimate pullout capacity of anchor plates increases with the embedment ratio but it reaches a constant value which is called the critical embedment ratio. Figure 3(b) presents the concept of the critical depth ratio. Beyond the critical embedment depth, the failure surface no longer reaches the ground surface, but is localized around the anchor. Ilamparuthi, Dickin, and Muthukrisnaiah (2002) and Tilak and Samadhiya (2021) showed experimentally that the presence of ground heave can be an indicator to separate the behavior of shallow and deep anchors.

A non-dimensional breakout factor, N_γ, is commonly adopted in the design of anchor plates in the sand as follows:

$$N_\gamma = \frac{Q_u}{\gamma A H} \qquad (6)$$

where Q_u is the ultimate pullout capacity of the anchor, γ is the soil unit weight, H is the embedment depth and A is the cross-section area of the anchor ($=\pi D^2/4$). In the present paper, the results of the analysis are presented in terms of N_γ.

3. Problem-solving algorithm

In solving the problem, a sequential approach involving the concept of passive zone, fan zone, and active zone is employed by using the method of stress characteristics. The passive zone, located adjacent to a known boundary, involves assuming a state of passive soil resistance to provide stability. Moving outward, the fan zone encompasses a region where both passive and active resistances contribute to load transfer. It assumes that the soil mobilizes its full shear strength and exhibits a nonlinear stress distribution. Finally, the active zone extends further away from the initial known boundary, and the analysis considers the soil as fully mobilized, exhibiting a linear stress distribution. By dividing the problem into these three zones, a step-by-step analysis can be conducted, gradually accounting for the increasing influence of the soil and determining the load transfer mechanism from the structure (anchor plate) to the surrounding soil. This sequential approach aids in
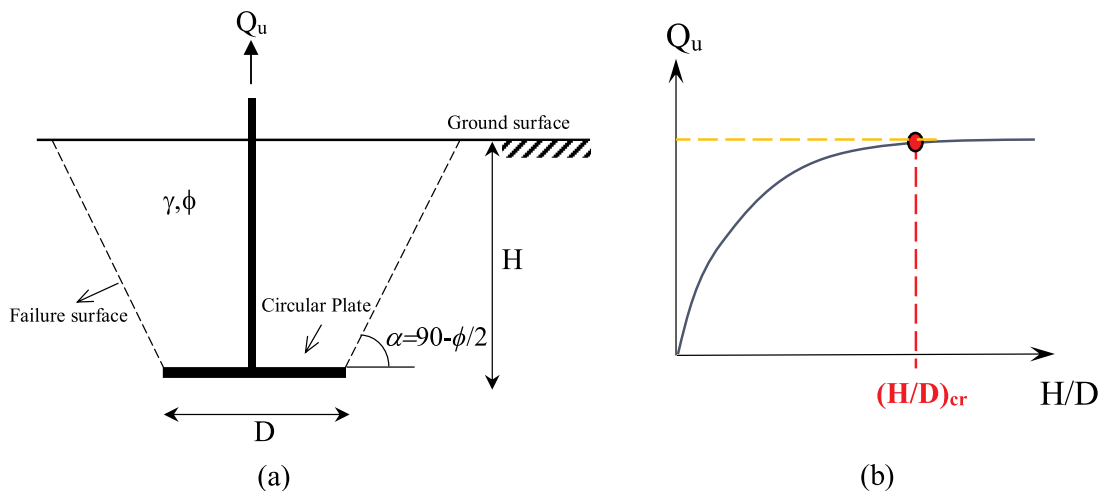
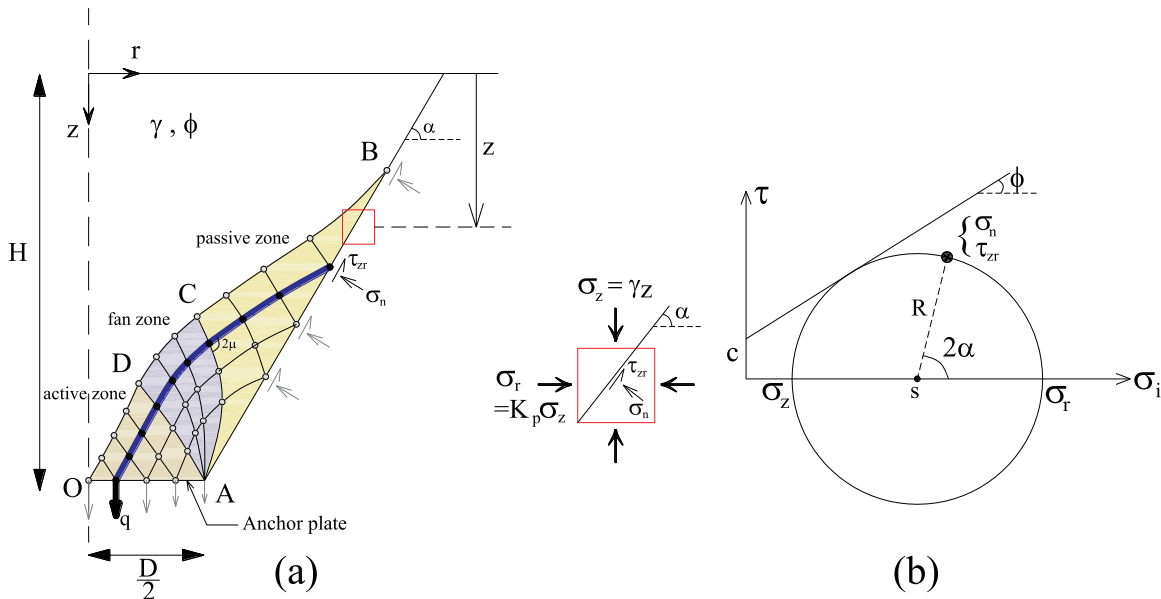Figure 3. A horizontal anchor plate definition concerning (a) geometry; (b) critical depth ratio.

Figure 4. Graphical definition of the problem and the solution approach (a) presentation of characteristic grid; (b) Mohr stress circle and components of an element over the boundary surface.

comprehending the complex soil-structure interaction and provides insights into the overall behavior and stability of the system.

By considering these three different zones, the domain is discretized into several α- and β- characteristics lines, called as characteristic grid or characteristic mesh, to solve boundary value problems governed by linear partial differential equations. The characteristic grid is constructed by selecting a set of characteristic curves that cover the problem domain, representing the paths along which information propagates. By transforming the governing equations into ordinary differential equations along these characteristic curves, the solution can be obtained by integrating along the grid lines of the characteristic grid. This grid-based approach enables the systematic evaluation of the solution at specific points or elements within the grid, allowing for the analysis of stress, displacement, or other relevant quantities.

A global scheme of the problem as well as the characteristic grid is depicted in Figure 4. Under the axisymmetric geometry of the problem, the analysis is performed only for one slice of the anchor plate. Different geometries of the anchor plates are considered by changing the H/D ratio (= 1 to 10) by keeping D a constant value (=0.5 m). Due to the soil homogeneity as well as the existence of soil unit weight as the only body force over the anchor, the problem solution is not dependent on the anchor dimension.

According to Figure 4(a), Points O and A are the center and the right edge of the plate, respectively. As can be seen, the soil on the plate is made up of three plastic areas that must be dissolved one after the other:

- Passive zone (ABC): Boundary conditions include coordinates and variables (r, z, σ and ψ) along non-characteristic line (AB) are known.
- Fan zone (ACD): Boundary conditions include known coordinates and variables (r, z, σ and ψ) along a characteristic line (AC) and point A itself.

- Active zone (ADO): Some boundary conditions include coordinates and variables (r, z, σ and ψ) along a characteristic line (AD), and other variables (like ψ) along the non-characteristic line (AO) are known.

The first known boundary of the problem is the non-characteristic line AB. The stress state of each point along this line can be calculated based on the principal stress components including the vertical and the lateral stress components of its representative element. The latter is assessed by using the lateral passive earth coefficient $K_p = \tan^2(45 + \phi/2)$. According to Figure 4(b), the shear (τ_{zr}) and normal (σ_n) stress components over the surface with the inclination angle of α can be assessed by applying the Mohr circle's rules.

The procedure for extending the characteristic grid in the passive, fan, and active zones is illustrated schematically in Figure 5. Initially, the first boundary line in the problem (Line AB), which is not a characteristic line, is discretized into a specific number of points labeled as nn. The α and β lines are denoted by blue and green colors, respectively, representing different sets of characteristic lines. It is important to note that the onset of the characteristic grid generation requires the repetition of selecting Point B to ensure the grid is formed along the entire length of the anchor plate, from Point A to Point O in Figure 4. The extension of the grid in each zone is explained as follows:

3.1. Passive zone solution

Two points 11 (i.e., Point A) and 22 on the known boundary line AB are considered at which, the stress components are already known. According to Figure 5(a), Point 12 is the intersection of two characteristic lines α and β that passes through points 11 and 22, respectively. Therefore, the coordinates of this point (12) are unknown and should be calculated. To find the coordinates (r,z) as well as the stress
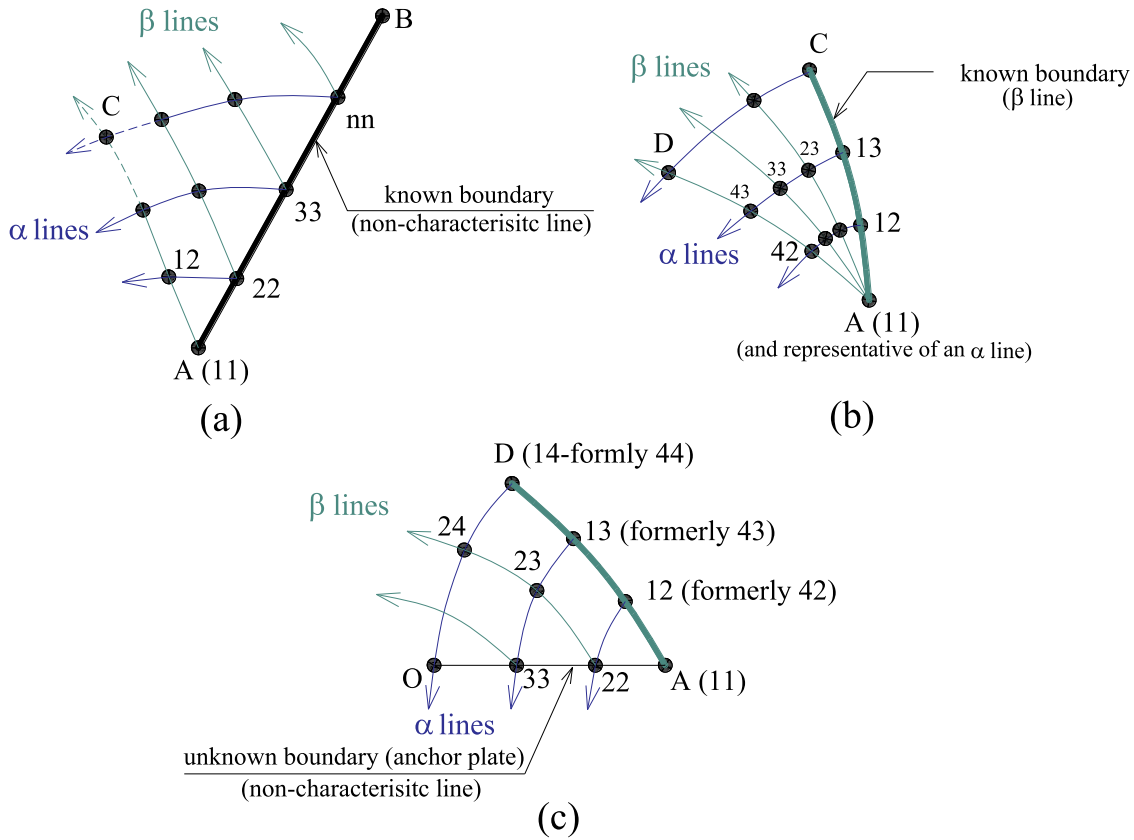
Figure 5. Extension of the characteristic grid through different zones for: (a) passive zone, (b) fan zone, (c) active zone.

variables (p,ψ) at point 12, it is enough to rewrite the system of Equations (4) and (5) in the approximate form of Equations (7) and (8) along α and β lines, respectively.

$$\frac{r_{12} - r_{11}}{z_{12} - z_{11}} = \tan\left[\frac{\psi_{12} + \psi_{11}}{2} - \mu\right] \quad (7.1)$$

$$(p_{12} - p_{11})\cos\phi - (R_{12} + R_{11})(\psi_{12} - \psi_{11})$$
$$+ \left(\frac{R_{12} + R_{11}}{r_{12} + r_{11}}\right)[\cos\phi(r_{12} - r_{11}) + (1 - \sin\phi)(z_{12} - z_{11})]$$
$$- \gamma[\cos\phi(z_{12} - z_{11}) + \sin\phi(r_{12} - r_{11})] = 0$$
$$(7.2)$$

$$\frac{r_{12} - r_{22}}{z_{12} - z_{22}} = \tan\left[\frac{\psi_{12} + \psi_{22}}{2} + \mu\right] \quad (8.1)$$

$$(p_{12} - p_{22})\cos\phi + (R_{12} + R_{22})(\psi_{12} - \psi_{22})$$
$$+ \left(\frac{R_{12} + R_{22}}{r_{12} + r_{22}}\right)[\cos\phi(r_{12} - r_{22}) - (1 - \sin\phi)(z_{12} - z_{22})]$$
$$- \gamma[\cos\phi(z_{12} - z_{22}) - \sin\phi(r_{12} - r_{22})] = 0$$
$$(8.2)$$

Finding the unknown variables of Point 12 (r_{12}, z_{12}, p_{12} and ψ_{12}) requires several trial and error calculations by solving Equations (7) and (8) simultaneously. The first initial estimate of the variables of Point 12 is placed in the set of Equations (8) and new values are found for the variables p_{12} and ψ_{12}. These values are then placed in the set of Equations (7) and new

values are found for the variables r_{12} and z_{12}. This operation is repeated until the required accuracy is achieved. The accuracy is defined as the relative error of two successive values of r_{12} and z_{12} which should be less than 0.01 for both of these parameters. Similar procedure is repeated for other points by moving in the direction of the known boundary line (AB) and the variables of other points (similar to Point 12) are assessed until all points inside the passive zone are obtained.

3.2. Fan zone solution

Unlike the passive zone where the information is only known on a non-specific line (AB), in the fan zone, the information of two α and β characteristic lines are known. As shown in Figure 5(b), the βline in the fan zone is AC while the α line is degenerated to a point (A) which means that all the points of the α line has the same variables (r,z,ψ,p). At the first point of this characteristic boundary (Point A or 11) that is a common line with the passive zone (line AC), the variables σ_{11} and ψ_{11} are known. Similarly, at the last point, which is common to the active zone, the variable ψ_{41} is zero. To obtain the specifications of other points in the fan zone, the same technique as explained in the previous section is applied.

3.3. Active zone solution

Having found the required data of the points in the fan zone, the coordinates (r,z) and the stress variables (p,ψ) along the last line of the α characteristic line (AD) are obtained. The line AO, which is representative of the anchor

plate, is a non-characteristic line along which, ψ is known. Since the calculation method is the same as other zones, the points are re-labeled. According to Figure 5(c), the variables of Point 22 are calculated from the information of Point 12 on the characteristic $\beta-$line (formerly named as 42) and from Point 11 on the line AO. Accordingly, it is possible to calculate the normal stress component over the anchor plate as the unknown boundary of the problem. Similarly, the variables of the interval Point 23 are obtained from the two Points 22 and 13. By implementing the same procedure used to solve the passive and fan zones, the unknown variables and normal stress components are obtained on different points along the anchor plate (line OA). Reminding that the grid generation is a repeating task, the characteristic grid will be accepted if the last line passes through Point O. Otherwise, a new grid is generated by selecting Point B with updated coordinates.

3.4. Pullout capacity assessment

The solution of simultaneous equations and the required calculations are performed by MATLAB programming platform. Based on the algorithm explained in the abovementioned sections, the stress state along the anchor plate is calculated at different points along the anchor plate. Due to the axisymmetric solution of the problem, the calculated normal stress along the anchor plate ($\sigma_{zi} = q_i$) at the point i corresponds to the value implemented over an annulus with the radius of r_i and the width Δr. Thus, the pullout capacity can be assessed by summing the incremental force (δQ_u) of this annulus for every point along the line OA as follows:

$$Q_u = \sum_i \delta Q_{ui} = \sum_i q_i (2\pi r_i)\Delta r \qquad (9)$$

4. Results and discussion

Characteristic grids are utilized here to investigate the behavior of circular anchor plates with varying embedment ratios as shown in Figure 6. The results demonstrate the influence of the embedment ratio with the values of H/D = 1, 2, 4, and 8 on the stress distribution (for $\phi=$ 30°). It is observed that for the shallow embedded anchor (H/D = 1), the starting point of the known boundary is situated at the ground surface; however, as the embedment ratio increases, the starting point of the known boundary shifts to greater depths. This shift is necessary to ensure that the grid is generated in a manner that the final characteristic line passes through the center of the circular anchor plate already represented by Point O in Figure 5.

Computation of the breakout factor N_γ has been performed based on Equations (6) and (9) for different values of $H/D = 1$ to 10 with intervals of one together with the soil friction angles of 25, 30, 35, 40, and 45 degrees. The variation of N_γ with the embedment ratio is depicted in Figure 7. It is observed that the N_γ value is not constant for an anchor plate situated in the soil with a specific ϕ, but it increases as the anchor plate is installed at deeper depths.

The growth in the N_γ value is not continuous with the increase of embedment ratio, but the value reaches an asymptote. Based on slope of the graphs, one can determine the critical embedment ratio ((H/D)$_{cr}$) beyond which, the N_γ value is almost constant. In Figure 7, the points corresponding to H/D$_{cr}$ are marked with red circles. By comparing the results for different soil friction angles, it is seen that the H/D$_{cr}$ is not the same for all the soil; bigger embedment ratios are obtained as the soil friction angle increases.

The breakout factor (N_γ) was computed using Equations (6) and (9) for a range of embedment ratios (H/D) from 1 to 10, with increments of one, while considering different soil friction angles of $\phi = 25, 30, 35, 40,$ and 45 degrees. The resulting variation of N_γ with the embedment ratio (H/D) is presented in Figure 7. Notably, the N_γ value is not a constant for anchor plates situated in soils with specific ϕ; rather, it demonstrates an increasing trend as the anchor plate is installed at deeper depths. This behavior indicates that deeper embedment leads to an enhanced breakout factor. However, the rate of increase in N_γ diminishes as the embedment ratio increases, ultimately reaching an asymptotic value. The graph provides insights into this trend, enabling the determination of the critical embedment ratio ((H/D)$_{cr}$) beyond which the N_γ value remains nearly constant. The red circles on Figure 7 highlight the corresponding points for the critical embedment ratio. Additionally, comparing the results for different soil friction angles reveals that (H/D)$_{cr}$ varies with the soil friction angle. Specifically, larger embedment ratios are achieved as the soil friction angle increases. This observation from the analyses suggests that the soil's friction angle has a significant influence on the critical embedment ratio and subsequently impacts the breakout factor of the anchor plate.

Following the N_γ-H/D graphs obtained in Figure 7, the critical embedment ratios are derived for different soil friction angles and the results are presented in Figure 8. It is observed that a linear variation exists between $\left(\frac{H}{D}\right)_{cr}$ and the soil friction angle (ϕ) with the relationship of $\left(\frac{H}{D}\right)_{cr} = 0.2\phi$ where ϕ is in degrees. To validate the obtained results, the critical embedment ratios from various analytical and experimental studies in the literature are also implemented in the same figure. A good agreement is observed among different experimental tests (Baker and Konder 1966; Clemence and Veesaert 1977; Esquivel-Diaz 1967; Ilamparuthi, Dickin, and Muthukrisnaiah 2002; Meyerhof and Adams 1968; Sutherland 1965; Tagaya, Scott, and Aboshi 1988; Tilak and Samadhiya 2021; Vesic 1971) and the analytical method in the present study.

To evaluate the obtained results, the breakout factor (N_γ) of this study is matched with that of other theoretical works in the literature. Figure 9 illustrates the variation of the breakout factor (N_γ) along with the embedment ratio in the range of 1 to 7 for soil friction angles of $\phi = 30°$ and 40°. In Figure 9(a), the results are compared with those of works based on the limit equilibrium method (Ghaly, Hanna, and Hanna 1991; Meyerhof and Adams 1968; Murray and Geddes 1987; Saeedy 1987). In the limit equilibrium method, a failure surface in the soil above the plate is assumed, along
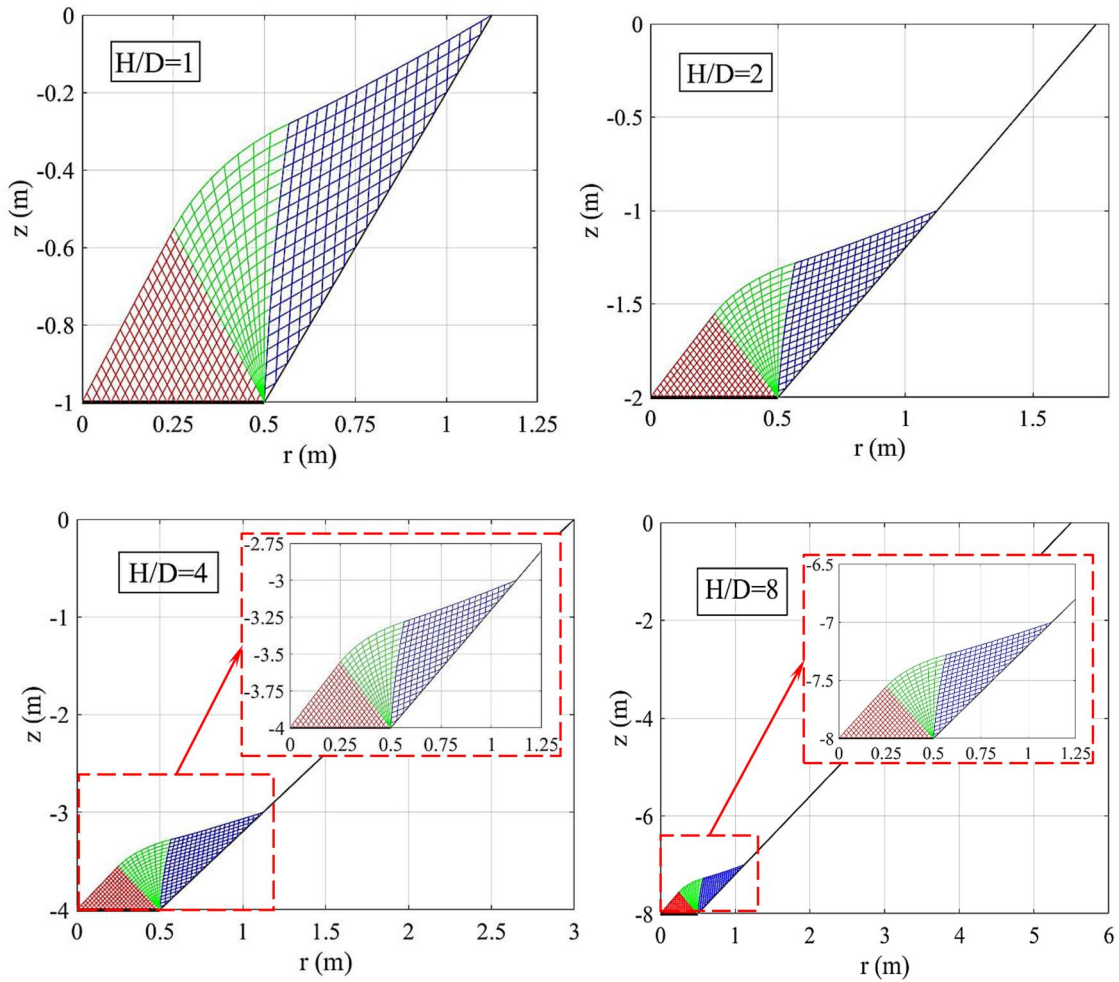
Figure 6. Presentation of the characteristic grid in the soil above the anchor plate for different embedment ratios (H/D = 1, 2, 4, and 8) with f = 30°.
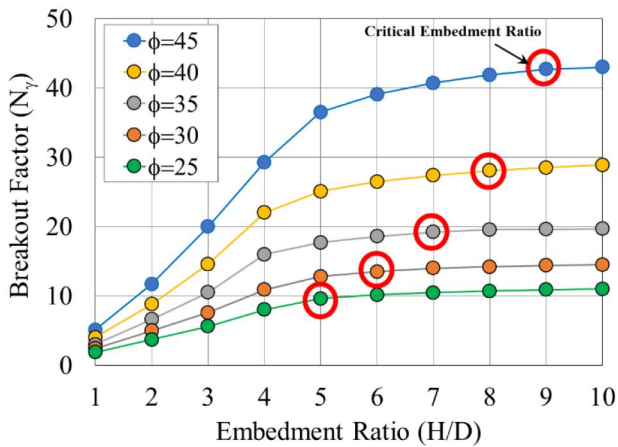

Figure 7. Variation of breakout factor (N_γ) with embedment ratio obtained for different soil friction angles.
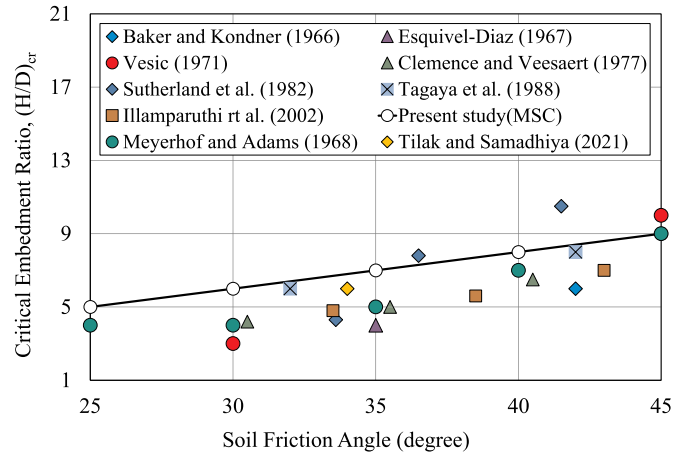

Figure 8. Variation of critical embedment ratio with soil friction angle obtained from this study and other works.

with a distribution of stress along this surface, and the pull-out force is calculated by satisfying equilibrium throughout the rigid soil body. Comparatively, the method of stress characteristics yields smaller solutions. In this method, a partial stress field extends to the entire body, satisfying equilibrium equations, yield criteria, and stress boundary conditions. However, it does not satisfy displacement compatibility conditions and, consequently, can be regarded

as a lower bound solution (Li and Jiang 2022; Yu 2007). A comparison of the results reveals that the breakout factor obtained in our study is lower than that in the works by Ghaly, Hanna, and Hanna (1991) and Murray and Geddes (1987), but higher than that of Saeedy (1987) and Meyerhof and Adams (1968). Notably, Ghaly, Hanna, and Hanna (1991) and Murray and Geddes (1987) assumed failure surfaces based on observed failure mechanisms of anchors in
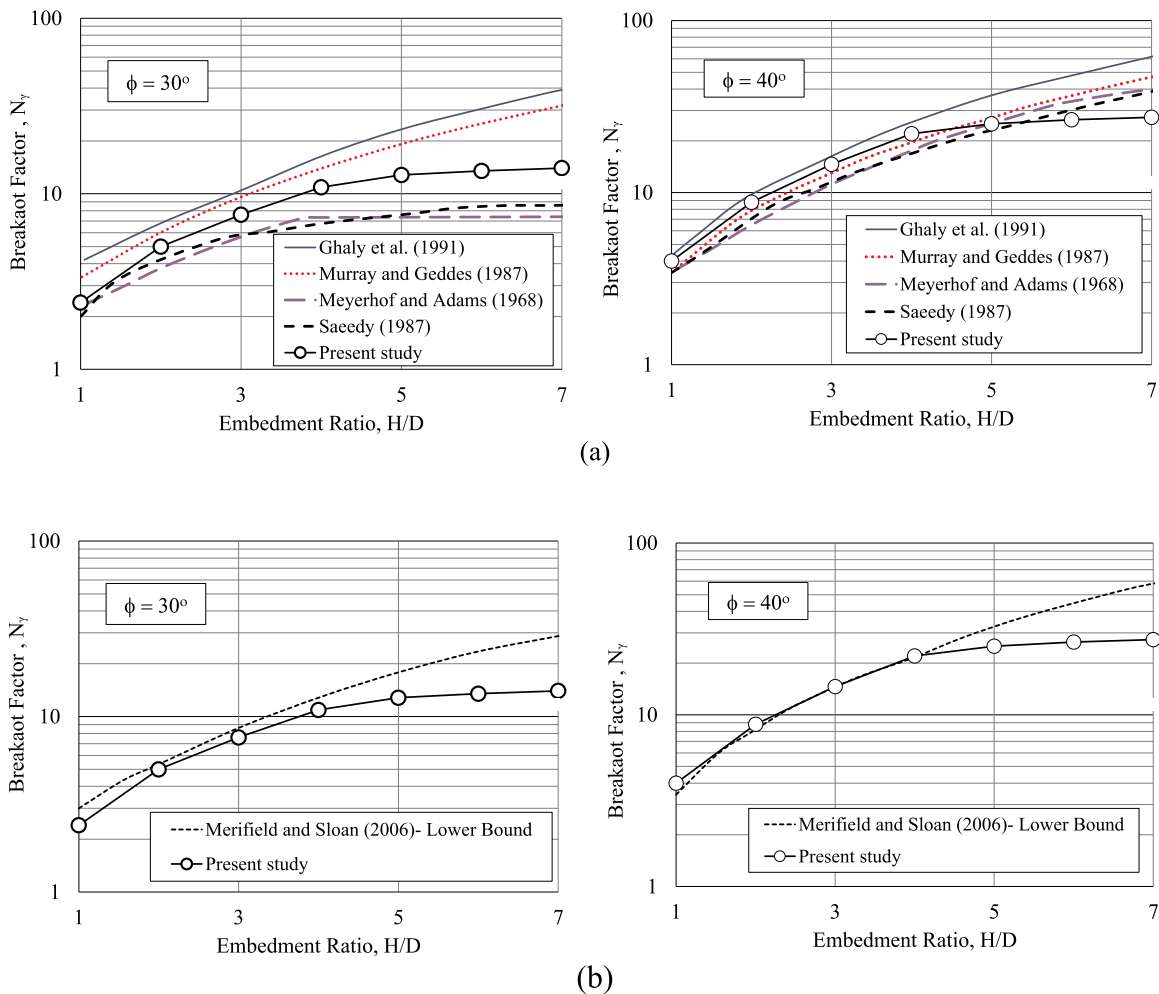
Figure 9. Comparison of the obtained results of this study with other analytical methods for $\phi = 30°$ and $40°$: (a) based on limit equilibrium method, (b) lower bound finite element method.

their experimental work and developed a mathematical model using the limit equilibrium method. In addition to the implementation of the limit equilibrium method, Saeedy (1987) and Meyerhof and Adams (1968) incorporated empirical factors to consider soil compaction and the shape factor. Despite the fact that the first two analytical works can be considered theoretical, the last two can be regarded as semi-theoretical. Figure 9(b) compares the results of this study with those of Merifield and Sloan (2006), who found the lower bound solution of N_γ using the numerical finite element method. They determined a statically admissible stress field in the soil that maximizes the collapse load over the anchor's area. A good match can be found between the two methods, especially for $H/D < 5$. Any observed differences can be attributed to the fundamental principles of the two methods, including the definition or absence of an assumed failure surface.

In addition to theoretical or semi-empirical solutions, there are a number of experimental works that investigated the pullout capacity of anchor plates. In these works, there is a diversity in the soil condition including gradation curve, particle geometry, and density, which reflects various soil shear strengths. It is noted that the only parameter reflecting the soil shear strength in this paper is the soil friction angle.

To gather all the results in a simple form, the results of several experimental works in the literature are compared together by considering the soil friction angle as the only parameter, and the results are classified into four groups with small ranges of soil friction angle of $\phi = 28 \sim 32°$, $\phi = 33 \sim 36°$, $\phi = 38 \sim 42°$ and $\phi = 42 \sim 45°$. The results are depicted in Figure 10. By comparing the results, a good match exists between the results from the method of stress characteristics and a wide range of experimental works (Adams and Hayes 1967; Baker and Konder 1966; Balla 1961; Clemence and Veesaert 1977; Ilamparuthi, Dickin, and Muthukrisnaiah 2002; Kananyan 1966; Kwasniewski, Sulikowska, and Walter 1975; Murray and Geddes 1987; Ovesen 1981; Sutherland 1965; Vesic 1971). It is found that for small values of ϕ ($28 \sim 32°$), the N_γ value is obtained higher a little bit from other works; however, for large ϕ values ($42 \sim 45°$), it seems that the N_γ is obtained as a lower bound value compared with other works. One exception exists for the mid value of ϕ ($= 33° \sim 36°$) where N_γ values of Tilak and Samadhiya (2021) was measured much smaller than other works. For large values of ϕ, it is also seen that the N_γ value obtained from this study reaches almost a constant value at $D/H \sim 9$ while it continues to rise and gets higher values. Based on this comparison, it can be
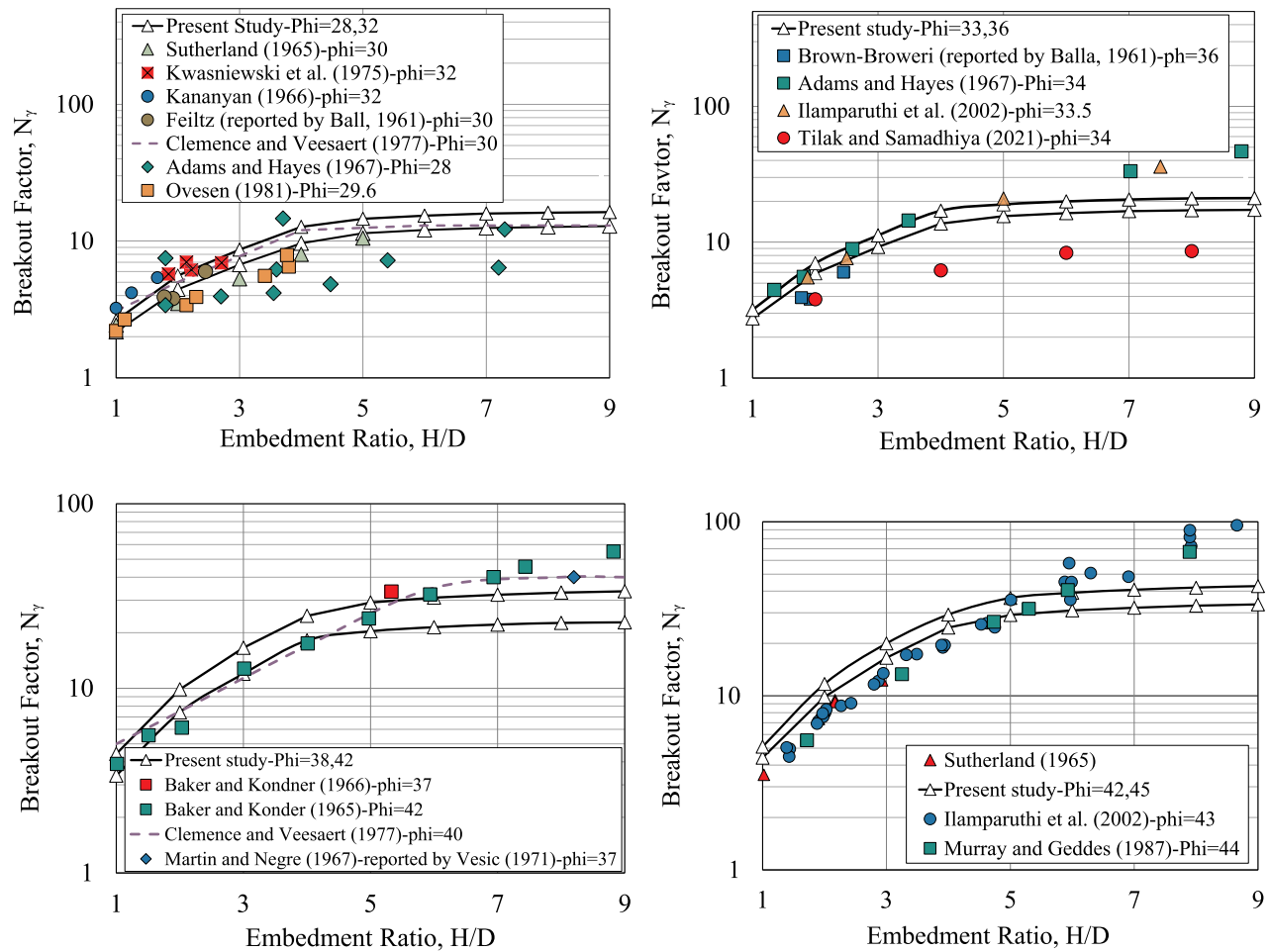
Figure 10. Comparison of the results of this study with those of laboratory experiments for different soil friction angles.

said that the results obtained using the method of stress characteristics are conservative or on the lower side when compared to both analytical methods and experimental works.

In addition to the specifications of the method of stress characteristics to be considered as a lower bound solution method, it is noted that to facilitate the analysis, certain assumptions were made in this study. Firstly, it was assumed that the soil friction angle and soil density remain constant at all depths. However, it should be noted that in actual field conditions and experimental tests, these properties may exhibit variations with depth. The assumption of constant soil properties simplifies the analysis but may deviate from real-world behavior. The potential impact of this assumption on the stress distribution and failure mechanisms around the anchor plate should be recognized and taken into consideration when interpreting the results. Future studies could explore more sophisticated approaches that incorporate depth-dependent soil properties to improve the accuracy of the analysis.

Another assumption made in this analysis is that the form of the failure surface in the soil above the anchor plate is considered as a line with a slope that varies as a function of the soil friction angle. It is important to note that this assumption is valid primarily for medium-depth installed

anchors. For deep anchors, the formation of a distinct failure surface might not occur, and instead, limited zones of localized deformation or stress concentration can develop (Hu et al. 2023; Liu, Liu, and Zhu 2012; Sabermahani and Shojaee Nasirabadi 2021). Therefore, the assumption of a constant failure surface for different embedment ratios should be interpreted with caution, particularly when analyzing deep anchor installations. Future research efforts could focus on investigating the behavior of deep anchors and incorporating more refined failure surface models that account for the localized deformation zones observed in practice. This would provide a more accurate representation of the stress distribution and load transfer mechanisms for deep anchor applications.

To enhance the practical applicability of the pullout capacity analysis for circular anchor plates in geotechnical engineering, an endeavor has been undertaken to develop a mathematical equation that expresses the magnitudes of the breakout factor (N_γ). By employing mathematical functions and employing curve fitting techniques through back analyses of the obtained data, a mathematical relationship is proposed in the form of Equation (10) as a function of embedment ratio (H/D) and soil friction angle (ϕ) in terms of degrees accompanied by the limitation defined by the critical embedment ratio:
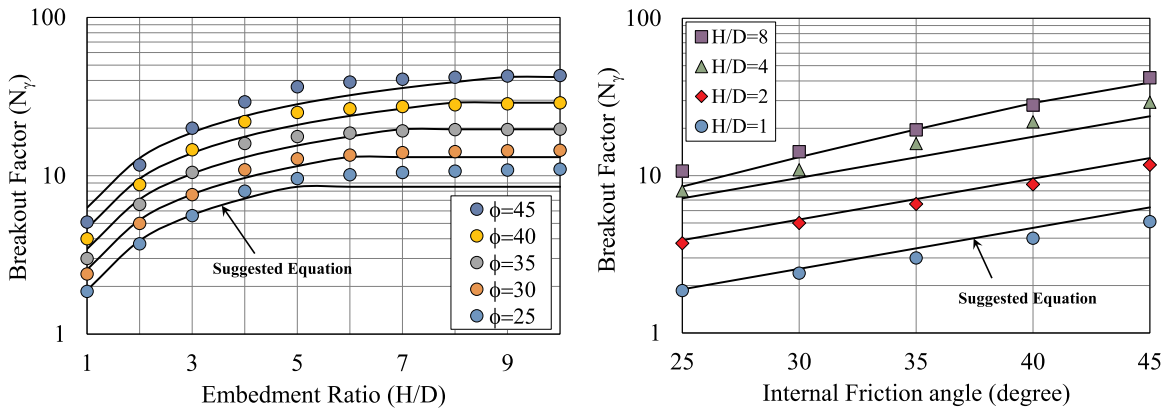
Figure 11. Breakout factor values from the results of this study with the proposed mathematical formulation in terms of: (a) embedment ratio; (b) internal friction angle.

$$N_\gamma = \frac{1.9(H/D)^{1.33}}{3.5 + H/D} e^{0.06\phi} \ for \ H/D \leq (H/D)_{cr}$$

$$= 0.2\phi(\phi = 25^o \sim 45^0) \qquad (10)$$

To assess the validity and practicality of Equation (10), the computed values of $N\gamma$, as determined by Equation (10), are juxtaposed with the results obtained using the method of stress characteristics. The resulting $N\gamma$ values are graphically depicted in Figure 11, illustrating their dependency on both the embedment ratio and soil friction angle. Upon comparison, it becomes evident that the proposed formulation broadly aligns with the observed trends in the analytical results. Notably, Equation (10) slightly underpredicts the N_γ value for friction angles of 25 and 45 degrees, particularly when $H/D = 4$. However, this prediction remains within an acceptable range. Consequently, this equation offers a quantitative framework for predicting the breakout factor, thereby facilitating the assessment of the pullout capacity of circular anchor plates in practical geotechnical engineering applications. It is important to note that this study solely utilizes the internal friction angle as a soil parameter to describe soil behavior. To enhance the practicality of the results, existing correlations in the literature, such as those with relative density, can be employed to predict the breakout factor.

5. Concluding remarks

In this study, the pullout capacity of horizontal circular anchor plates was analyzed using the method of stress characteristics. The findings and discussions presented throughout this paper shed light on the behavior and performance of horizontal circular anchor plates under varying embedment ratios. Through comprehensive numerical simulations and back analyses of experimental data, several key insights have been obtained.

Firstly, the method of stress characteristics has proven to be a valuable tool in estimating the pullout capacity of circular anchor plates. It offers a systematic approach to analyzing the stress distribution and load transfer mechanisms, providing valuable engineering insights. The use of characteristic grids allowed for the visualization and interpretation

of stress patterns, aiding in the understanding of the plate-soil interaction behavior.

Secondly, the assumption of a constant soil friction angle and density, though simplifying the analysis, should be considered in light of its limitations. The variability of soil properties with depth was not considered in this study, which may influence the accuracy of the results. Future research could explore the incorporation of depth-dependent soil properties to refine the analysis.

Additionally, the assumption of a constant failure surface for different embedment ratios may not capture the complex behavior observed in deep anchor installations. The presence of limited zones and the disappearance of distinct failure surfaces necessitate further investigation and the development of refined failure surface models.

Furthermore, a mathematical equation has been derived to express the magnitudes of the breakout factor, enhancing the practical applicability of the analysis in geotechnical engineering. This equation provides a valuable tool for estimating the breakout factor and facilitating the prediction and assessment of circular anchor plate pullout capacity.

In conclusion, this study has contributed to the understanding of circular anchor plate behavior and the application of the method of stress characteristics. The insights gained from this research can inform design and analysis practices in geotechnical engineering, aiding in the efficient and reliable use of horizontal circular anchor plates for various soil friction angles. However, further research is recommended to refine the analysis by considering depth-dependent soil properties and investigating the behavior of deep anchor installations. Such advancements will enhance the accuracy and applicability of the method in practical engineering problems.

Acknowledgements

Disclosure statement

ORCID

Ehsan Seyedi Hosseininia http://orcid.org/0000-0002-9810-8698

References

Adams, J. I., and D. C. Hayes. 1967. The Uplift Capacity of Shallow Foundations. *Ontario Hydro Research Quarterly* 19 (1): 1–15.

Al Hakeem, Nabil, and Charles Aubeny. 2019. Numerical Investigation of Uplift Behavior of Circular Plate Anchors in Uniform Sand. *Journal of Geotechnical and Geoenvironmental Engineering* 145 (9): 04019039. https://doi.org/10.1061/(ASCE)GT.1943-5606.0002083

Baker, W.H., and R.L. Konder. 1966. Pullout load capacity of a circular earth anchor buried in sand. National Academy of Sciences, *Highway Research Record* 108, 1–10.

Balla, A. 1961. The Resistance to Breaking-Out of Mushroom Foundations for Pylons. Paper presented at the Proceeding of 5th International Conferences on SMFE.

Bolton, M. D., and C. K. Lau. 1993. Vertical Bearing Capacity Factors for Circular and Strip Footings on Mohr Coulomb Soil. *Canadian Geotechnical Journal* 30 (6): 1024–1033. https://doi.org/10.1139/t93-099

Cassidy, M. J., and G. T. Houlsby. 2002. Vertical Bearing Capacity Factors for Conical Footings on Sand. *Géotechnique* 52 (9): 687–692. https://doi.org/10.1680/geot.2002.52.9.687

Clemence, S. P., and C. J. Veesaert. 1977. Dynamic Pullout Resistance of Anchors in Sand. Paper Presented at the Proceedings of the International Symposium on Soil-Structure Interaction.

Cox, A. D. 1962. Axially Symmetry Plastic Deformation in Soils. II. Indentation of Ponderable Soils. *International Journal of Mechanical Sciences* 4 (5): 371–380. https://doi.org/10.1016/S0020-7403(62)80024-1

Cox, A. D., G. Eason, and H. G. Hopkins. 1961. Axially Symmetric Plastic Deformation in Soils. *Philosophical Transactions of the Royal Society of London, Series A* 254: 1–45.

Dickin, E. A., and C. F. Leung. 1983. Centrifugal Model Tests on Vertical Anchor Plates. *Journal of Geotechnical Engineering* 109 (12): 1503–1525. https://doi.org/10.1061/(ASCE)0733-9410(1983)109:12(1503)

Dickin, Edward A. 1988. Uplift Behavior of Horizontal Anchor Plates in Sand. *Journal of Geotechnical Engineering* 114 (11): 1300–1317. https://doi.org/10.1061/(ASCE)0733-9410(1988)114:11(1300)

Esquivel-Diaz, Raul F. 1967. Pullout Resistance of Deeply Buried Anchors in Sand. *Duke University*.

Ganesh, R., and Jagdish Prasad Sahoo. 2019. Vertical Uplift Capacity of a Group of Shallow Circular Plate Anchors in Sand. *Marine Georesources & Geotechnology* 37 (3): 282–290. https://doi.org/10.1080/1064119X.2017.1410868

Ghaly, Ashraf, Adel Hanna, and Mikhail Hanna. 1991. Uplift Behavior of Screw Anchors in Sand. I: Dry Sand. *Journal of Geotechnical Engineering* 117 (5): 773–793. https://doi.org/10.1061/(ASCE)0733-9410(1991)117:5(773)

Haar, A., and T. von Kármán. 1909. Zur Theorie der Spannungszustände in plastischen und sandartigen Medien. *Nachr. Königl. Ges.Wiss*: 204–218.

Hill, R. 1950. *The Mathematical Theory of Plasticity*. Oxford: Clarendon press.

Hu, Shihong, Lianheng Zhao, Yigao Tan, Yibo Luo, and Zhonglin Zeng. 2022. Three-Dimensional Upper-Bound Limit Analysis of Ultimate Pullout Capacity of Anchor Plates Using Variation Method. *International Journal for Numerical and Analytical Methods in Geomechanics* 46 (7): 1356–1379. https://doi.org/10.1002/nag.3349

Hu, Wei., Zhi Lin, Hui Wang, Pu Zhao, Dongxue Hao, and Jian Gong. 2023. Method for Calculating the Uplift Capacity of a Circular Anchor Plate at Arbitrary Depth in Sand. *SSRN*. https://doi.org/10.2139/ssrn.4383384

Ilamparuthi, K., E. A. Dickin, and K. Muthukrisnaiah. 2002. Experimental Investigation of the Uplift Behaviour of Circular Plate Anchors Embedded in Sand. *Canadian Geotechnical Journal* 39 (3): 648–664. https://doi.org/10.1139/t02-005

Kanakapura, S., S. Rao, and J. Kumar. 1994. Vertical Uplift Capacity of Horizontal Anchors. *Journal of Geotechnical Engineering* 120 (7): 1134–1147. https://doi.org/10.1061/(ASCE)0733-9410(1994)120:7(1134)

Kananyan, A. S. 1966. Experimental Investigation of the Stability of Bases of Anchor Foundations. *Soil Mechanics and Foundation Engineering* 3 (6): 387–392. https://doi.org/10.1007/BF01702954

Kumar, J. 2006. Uplift Response of Strip Anchors in Sand Using FEM. *Iranian Journal of Science & Technology, Transaction B, Engineering* 30 (B4): 475–486.

Kumar, Jyant, and Priyanka Ghosh. 2005. Bearing Capacity Factor N_γ for Ring Footings Using the Method of Characteristics. *Canadian Geotechnical Journal* 42 (5): 1474–1484. https://doi.org/10.1139/t05-051

Kwasniewski, J., I. Sulikowska, and A. Walter. 1975. Anchors with Vertical Tie Rods. Paper Presented at the Proceedings of the 1st Baltic Conference, Soil Mechanics and Foundation Engineering, Gdansk, Poland.

Larkin, L. A. 1968. Theoretical Bearing Capacity of Very Shallow Fotings. *ASCE. Journal of the Soil Mechanics and Foundations Division* 94 (6): 1347–1357. https://doi.org/10.1061/JSFEAQ.0001200

Li, Chengchao, and Pengming Jiang. 2022. Method of Rigorous Characteristics for Seismic Bearing Capacity of Strip Footings Placed Adjacent to Homogeneous Soil Slopes. *International Journal of Geomechanics* 22 (10): 04022179. https://doi.org/10.1061/(ASCE)GM.1943-5622.0002526

Liang, Weijian, Jidong Zhao, Huanran Wu, and Kenichi Soga. 2021. Multiscale Modeling of Anchor Pullout in Sand. *Journal of Geotechnical and Geoenvironmental Engineering* 147 (9): 04021091. https://doi.org/10.1061/(ASCE)GT.1943-5606.0002599

Liu, Jinyuan, Mingliang Liu, and Zhende Zhu. 2012. Sand Deformation around an Uplift Plate Anchor. *Journal of Geotechnical and Geoenvironmental Engineering* 138 (6): 728–737. https://doi.org/10.1061/(ASCE)GT.1943-5606.0000633

Mariupol'skii, L. G. 1965. The Bearing Capacity of Anchor Foundations. *Soil Mechanics and Foundation Engineering* 2 (1): 26–32. https://doi.org/10.1007/BF01704424

Merifield, Richard S., and Scott W. Sloan. 2006. The Ultimate Pullout Capacity of Anchors in Frictional Soils. *Canadian Geotechnical Journal* 43 (8): 852–868. https://doi.org/10.1139/t06-052

Merifield, R. S., A. V. Lyamin, and S. W. Sloan. 2006. Three Dimensional Lower Bound Solutions for the Stability of Plate Anchors in Sand. *Géotechnique* 56 (2): 123–132. https://doi.org/10.1680/geot.2006.56.2.123

Meyerhof, G. G., and J. I. Adams. 1968. The Ultimate Uplift Capacity of Foundations. *Canadian Geotechnical Journal* 5 (4): 225–244. https://doi.org/10.1139/t68-024

Mitsch, M.P., and S. P. Clemence. 1985. The uplift capacity of helix anchors in sand. In *Uplift behavior of anchor foundations in soil*, edited by ASCE, 26–47. Michigan: ASCE.

Mittal, Satyendra, and Sanjeev Mukherjee. 2014. Vertical Pullout Capacity of a Group of Helical Screw Anchors in Sand: An Empirical Approach. *Indian Geotechnical Journal* 44 (4): 480–488. https://doi.org/10.1007/s40098-014-0099-1

Mohammadkhanifard, HamidReza, Matin Jalali Moghadam, Amirali Zad, and MohammadHasan Ramesht. 2022. Evaluating the Behavior of Expandable Multi-Plate Mechanical Anchors in Granular Soils. *Marine Georesources & Geotechnology* 40 (10): 1205–1223. https://doi.org/10.1080/1064119X.2021.1980638

Mokhbi, Hicham, Mekki Mellas, Abdelhak Mabrouki, and Jean-Michel Pereira. 2018. Three-Dimensional Numerical and Analytical Study of Horizontal Group of Square Anchor Plates in Sand. *Acta Geotechnica* 13 (1): 159–174. https://doi.org/10.1007/s11440-017-0557-x

Murray, E. J., and James D. Geddes. 1987. Uplift of Anchor Plates in Sand. *Journal of Geotechnical Engineering* 113 (3): 202–215. https://doi.org/10.1061/(ASCE)0733-9410(1987)113:3(202)

Ovesen, N. K. 1981. Centrifuge Tests of the Uplift Capacity of Anchors. Paper Presented at the Proceedings of the 10th

International Conference on Soil Mechanics and Foundation Engineering, Stockholm.

Rowe, R. K., and E. H. Davis. 1982. Behaviour of Anchor Plates in Sand. *Géotechnique* 32 (1): 25–41. https://doi.org/10.1680/geot.1982.32.1.25

Sabermahani, Mohsen, and Mehrzad Shojaee Nasirabadi. 2021. Vertical Uplift Resistance of an Innovative Plate Anchor Embedded in Sand. *Marine Georesources & Geotechnology* 39 (7): 842–858. https://doi.org/10.1080/1064119X.2020.1773590

Saeedy, Hamed S. 1987. Stability of Circular Vertical Earth Anchors. *Canadian Geotechnical Journal* 24 (3): 452–456. https://doi.org/10.1139/t87-056

Sokolovski, V. V. 1965. Statics of Granular Media. 1st ed. Pergamon Press, Oxford eBook.

Sutherland, H. B. 1965. Model Studies for Shaft Raising Through Cohesionless Soils. Paper presented at the Proceeding of the Soil Mechanics & Foundation Engineering Conference, Canada.

Tagaya, Kozo, Ronald F. Scott, and Hisao Aboshi. 1988. Pullout Resistance of Buried Anchor in Sand. *Soils and Foundations* 28 (3): 114–130. https://doi.org/10.3208/sandf1972.28.3_114

Tilak, B. Vidya, and Narendra Kumar Samadhiya. 2021. Pullout Capacity of Multi-Plate Horizontal Anchors in Sand: An Experimental Study. *Acta Geotechnica* 16 (9): 2851–2875. https://doi.org/10.1007/s11440-021-01173-1

Vesic, Aleksandar S. 1971. Breakout Resistance of Objects Embedded in Ocean Bottom. *Journal of the Soil Mechanics and Foundations Division* 97 (9): 1183–1205.

Xing, Guoqi, Lijun Zhang, Yupeng Cao, Wei Xuan, Xiaotong Zhang, and Rong Wang. 2023. Failure Criterion of Double-Plate Vertically Loaded Anchor in Saturated Marine Fine Sand under Monotonic Loading. *Marine Georesources & Geotechnology* 41 (6): 620–633. https://doi.org/10.1080/1064119X.2022.2079034

Yu, Hai-Sui. 2007. *Plasticity and Geotechnics*. Vol. 13. Springer: Springer Science & Business Media.

Zhang, Nan., T. Matthew Evans, Shiwei Zhao, Yu Du, and Lei Zhang. 2020. Discrete Element Method Simulations of Offshore Plate Anchor Keying Behavior in Granular Soils. *Marine Georesources & Geotechnology* 38 (6): 716–729. https://doi.org/10.1080/1064119X.2019.1614705

Zhang, Ning, Huai-Na Wu, Jack Shui-Long Shen, Takenori Hino, and Zhen-Yu Yin. 2017. Evaluation of the Uplift Behavior of Plate Anchor in Structured Marine Clay. *Marine Georesources & Geotechnology* 35 (6): 758–768. https://doi.org/10.1080/1064119X.2016.1240273

Zhao, L. H., L. Li, F. Yang, and X. Liu. 2011. Joined Influences of Nonlinearity and Dilation on the Ultimate Pullout Capacity of Horizontal Shallow Plate Anchors by Energy Dissipation Method. *International Journal of Geomechanics* 11 (3): 195–201. https://doi.org/10.1061/(ASCE)GM.1943-5622.0000075